ISSN: 2458-8989

Natural and Engineering Sciences

NESciences, 2025, 10 (3): 67-84 doi: 10.28978/nesciences.1811107

Inorganic Geochemistry Study of Carbonate Components in Two Sections, Sargelu Formation, Northeast Iraq

Farhad Ahmed Mohammad [1*], Dashti Arf. Suliaman [2]

[1*] Department of Earth Sciences and Petroleum, College of Science, Salahaddin University, Erbil, Kurdistan Region, Iraq. E-mail: farhad.mohammad@su.edu.krd

[2] Chemical and Petrochemical Department, Engineering College, Salaheddin University, Erbil, Iraq. E-mail: dashti.sulaiman@su.edu.krd

Abstract

The Sargelu Formation (Middle Jurassic) is very widespread in Iraq and neighboring states. This paper will address two portions of the formation, Barzewa and Barsamarin, which are found within the Erbil Governorate, in northern Iraq. The main objective is to study the mineralogical make-up, geochemical features, and setting up of the Sargelu Formation. These sections gave 21 carbonate component samples that were examined through the use of X-ray diffraction (XRD), Fourier transform infrared (FTIR) spectroscopy, and Scanning Electron Microscopy (SEM). Findings demonstrate that the significant mineral constituents include calcite, dolomite, quartz, and clay minerals, with carbonate minerals mainly comprising euhedral and anhedral calcite and dolomite. Geochemical analysis reveals an Al_2O_3/TiO_2 ratio of 17.39, suggesting an intermediate source rock composition. The depositional environment of the Sargelu Formation is interpreted as shallow marine to marine on sea ramps, based on the V vs. Al_2O_3 diagram and the presence of coccoliths observed under SEM. Coccoliths, which are abundant in the sunlight zone of the ocean, confirm the marine origin of the deposits. This paper gives a comprehensive description of the Sargelu Formation, with its mineralogical and geochemical features that are essential to learn about its formation history and its future prospects as a hydrocarbon storage. The results add to the general knowledge about the Jurassic stratigraphy in Kurdistan.

Keywords:

Coccoliths, earth science, environmental science, geochemistry, marine carbonates, sargelu formation.

Article history:

Received: 02/06/2025, Revised: 22/07/2025, Accepted: 21/08/2025, Available online: 12/12/2025

**Corresponding Author: Farhad Ahmed Mohammad, E-mail: farhad.mohammad@su.edu.krd*

Introduction

The Sargelu Formation is one of the primary units of the Middle Jurassic that is known to be significant as a source of hydrocarbons in the deposit and in the immediate surroundings of Iraq (Jassim & Goff, 2006; He et al., 2011). Especially the Barzewa and Barsarin areas of the Erbil Governorate in northeast Iraq are unique with the preserved carbonate-rich strata (Punam & Patel, 2025; Pitman et al., 2004). These parts are a unique chance to investigate mineralogical and geochemical peculiarities of the formation, which is mainly represented by dark grey limestone with punctual shale (Al-Ameri & Al-Nagshbandi, 2015). The depositional setting of the Sargelu Formation is mostly shallow to marine (Srinivas & Rajesh, 2025), and such areas offer a significant setting to study the mineral content and geochemical characteristics that make the formation so important in the formation of a hydrocarbon source rock (Abdula et al., 2015; Punam & Patel, 2026). As indicated in Figure 1, the Barzewa section is near the Barzewa Village (Latitude: 38S 0475516, Longitude: 4041633), whereas Barsarin is close to the Balak River in the Barsarin Village (Latitude: 38S 0467792, Longitude: 4054787).

Figure 1. Google earth map showing the barzewa and barsarin location, which is situated in the ne of erbil governorate

The primary purpose of the proposed research is to examine the mineralogical and geochemical data on the mineral components of carbonates in the Sargelu Formation, namely, in the sections of Barzewa and Barsarin (Chatterjee & Singh, 2023; Beydoun et al., 1992). The proposed study will enrich the knowledge on the depositional environment, provenance, and mineral composition of the formation through a critical evaluation of the mineral composition and geochemical data. It is accomplished through the use of high precision analytical methods, such as X-ray diffraction (XRD), Fourier-Transform infrared spectroscopy (FTIR), and Scanning Electron Microscopy (SEM) to give a detailed analysis of the carbonate minerals, mainly calcite and dolomite, and the geochemical signatures of these minerals (Al-Ameri & Zumberge, 2012; Hakimi et al., 2015).

Despite the Sargelu Formation being identified as a significant hydrocarbon source rock, not much is known of the depositional environment, mineralogical composition, and provenience in the Barzewa and Barsarin fields. This gap is what this paper attempts to fill by researching the alteration of the composition of carbonate stones and the quantity of trace elements that would assist in determining the paleoenvironment in the time period when the formation was deposited (Al-Ameri & Zumberge, 2012; Hakimi et al., 2015). The first hypothesis used in this work is that the Sargelu Formation in Barzewa and Barsarin sections is principally made of shallow marine carbonates, and the mineralogical composition indicates that there must be an

intermediate source (Majdanishabestari & Soleimani, 2019). The hypothesis in the study is also that geochemical differences within these sections can be attributed to depositional environment (Mousa, 2022) and environmental conditions in the region throughout the Middle Jurassic (Ganesan et al., 2024).

The study will make valuable contributions to the structure of the Sargelu Formation by providing a careful study of the carbonate contents in the Barzewa and Barsarin sections. One of the most important contributions of the study is that it used sophisticated geochemical techniques to determine the depositional setting, provenience, and mineralogy of the Sargelu Formation. Through the analysis of the trace elements and rare earth elements, a new insight into the source rocks of the formation and geological history is to be provided (Al-Ameri & Zumberge, 2012; Dai et al., 2015). Also, the evidence of the mineral morphology, relying on the analysis of SEM, gives further contribution to the reconstruction of the environment of deposition and its marine impact. This research is crucial for enhancing the geological and petroleum exploration potential of the region (Kownacki et al., 2015).

The paper has the following structure: it is divided into a Geological Situation, whereby the stratigraphy and geographical positioning of the Sargelu Formation in the Kurdistan Region are explained (Jassim & Goff, 2006). This is then succeeded by the Materials and Methods section, where the sampling places and the methods used to conduct the analysis are described. The results section describes the mineralogical and geochemical results and is backed by figures and tables that depict the mineral composition and the trace elements and rare earth elements data. The results are discussed to provide insight into the provenance, depositional environments, and the implications of the hydrocarbon potential of the formation. Lastly, the Conclusion is where the most important results are summarized and where the significance of the Sargelu Formation and its further agenda in geological and petroleum research is highlighted (Al-Ameri & Zumberge, 2012; Van Bellen & Dunnington, 1959).

Geological Setting

The Sargelu Formation is seen in several outcrops and localities in the Iraqi Kurdistan Region (Jassim & Goff, 2006). The Arabian plate, together with the adjacent blocks of Turkish and Iranian continental parts, constituted part of the long-passive plate boundary of Gondwanaland during the Paleozoic (570-245 Ma) and was connected to Africa (Beydoun, 1986; Beydoun et al., 1992). The Arabian portion of Gondwanaland (collectively known as the Cimmerian blocks) was separated by extension and rifting during the middle Permian and the Triassic to Jurassic (250 Ma to 160 Ma). With the opening of the Neo-Tethys Ocean, the Arabian part microplates sank to the formation of the so-called Arabian Promontory.

In addition, oceanic Arabian Plate crust under the Eurasian Plate resulted in collisions of continental parts of the Eurasian margin with the continental Arabian Plate, which formed the Zagros Mountains. This continent-to-continent collision began in the late Eocene and continues to this day (Beydoun, 1985).

The global sea level rise during the Middle Jurassic led to the deposition of these sediments in an open-marine environment. Neo-Tethys was now flanked by the Arabian Plate (AP) as its passive edge to the north and northeast direction. As a result, north of Iraq, which includes the Sargelu Formation, is situated in the northeastern region of the Arabian tectonic Plate (Martin, 2001).

Materials and Methods

In the fall of 2022, fieldwork was carried out on the Sargelu Formation. This study was done on two outcrops in the Imbricated Zone of the Erbil Governorate in the villages of Barzewa and Barsarin. Columnar drawings

were made for both sections (Figure 2 A&B). A total of 21 fresh carbonate shale rock samples were collected, 11 from the Barzewa section and 10 from the Barsarin section. These samples were taken from the area between the top contact (Naokelekan Formation) and the lower part of the Sargelu Formation.

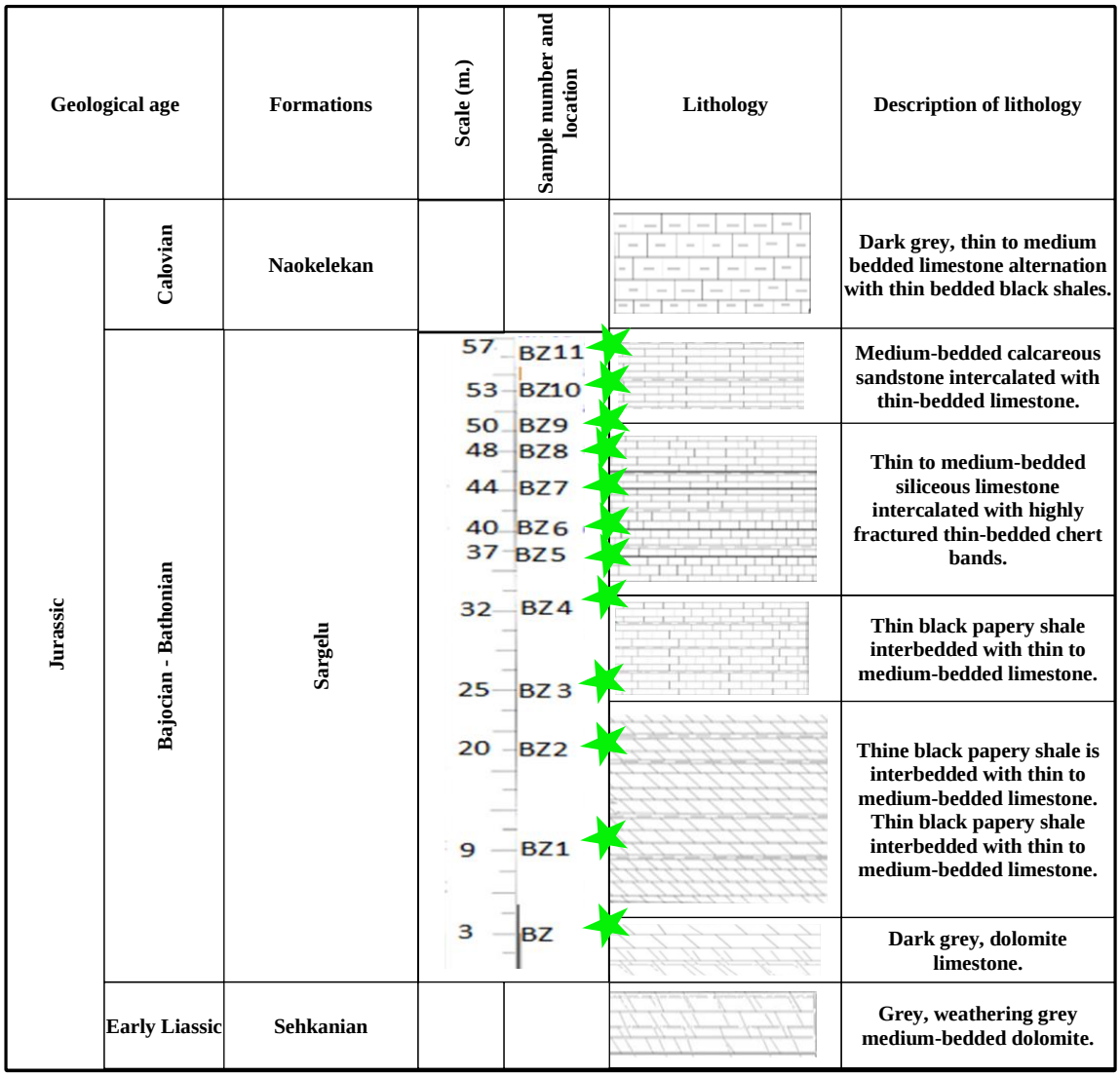

Figure 2A. Lithological column of the barzewa section (bz) showing the stratigraphic succession of the sargelu formation

The column illustrates the lithological characteristics, sample numbers, and stratigraphic positions within the Barzewa section. The Sargelu Formation, of Bajocian–Bathonian age, is underlain by the Sehkanian Formation (Early Liassic) and overlain by the Naokelekan Formation (Callovian). The lithology consists mainly of dark grey, thin- to medium-bedded limestones interbedded with black shales and calcareous sandstones. Sampling locations (BZ1–BZ10) are indicated along the column.

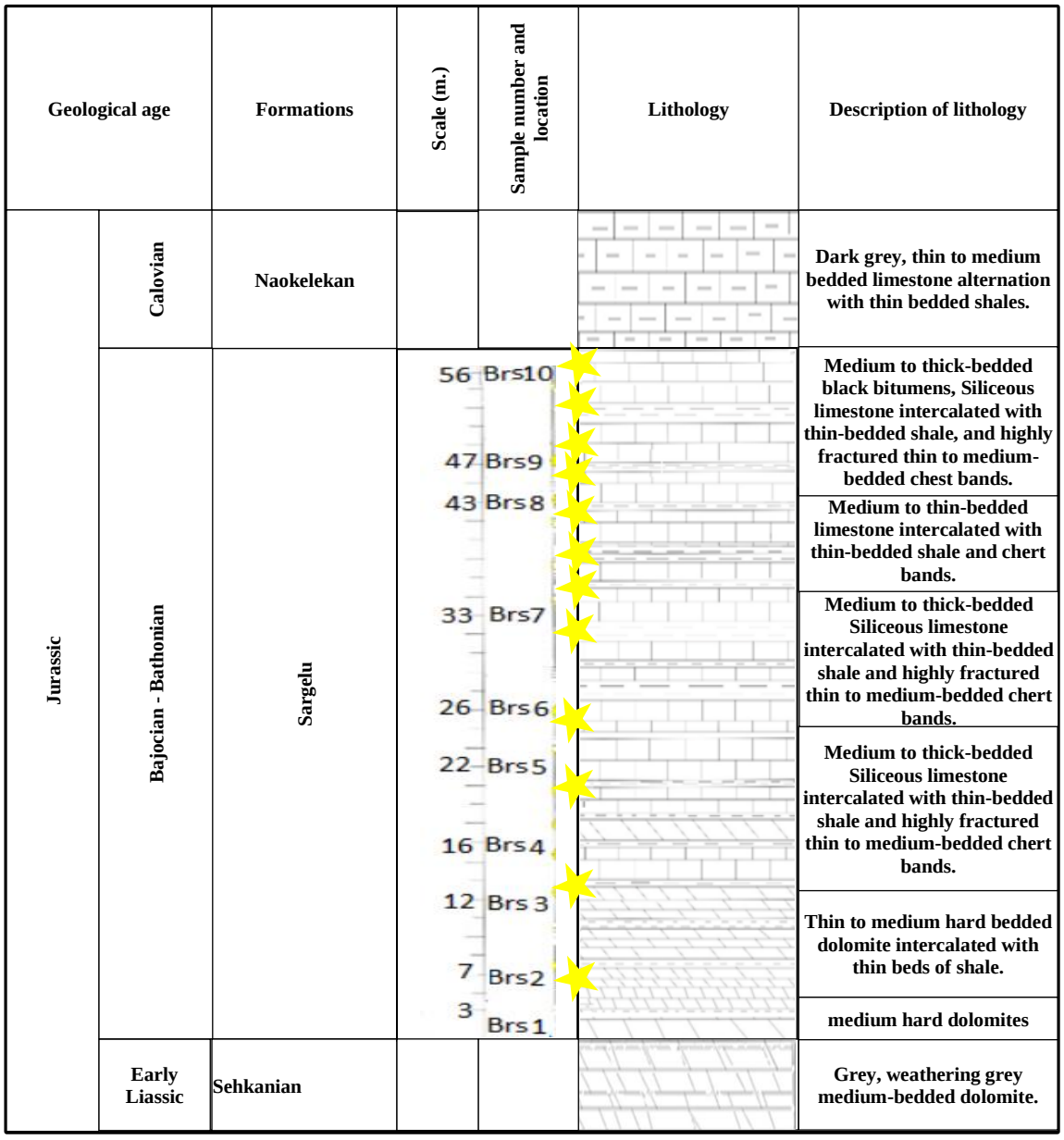

Figure 2B. Columnar stratigraphic section of the barsirin outcrop (Brs)

The illustration above shows the Lithological Profile of the Sargelu Formation and Sample Locations. The unit is located between the underlying Naokelekan Formation (Calovian) and the Bajocian-Bathonian Sargelu Formation, which demonstrates different lithological units, i.e., medium and thick-bedded siliceous limestone intercalated with thin-bedded shale and chert bands, and medium-hard dolomite. The positions of the samples (Brs1-Brs10) are marked on the column, which allows documenting the stratigraphy and lithology of the Barsirin part of the formation.

To analyze the mineral content, bulk sample powders and clay fractions were examined using X-ray diffraction (XRD). Clay fractions were prepared by removing organic materials with 30% H2O2, washing with distilled water, drying, and placing the samples on glass slides.

Each sample was prepared as one untreated slide and one treated with ethylene glycol vapor at 60°C for one hour. Also, three samples were heated at 550°C for three hours. The bulk materials and clay fractions

were analyzed using the Sintag PAD V X-ray diffractometer (with a Ni-filtered Cu-Kalpha 40 kV and 30 mA). The primary oxides were also examined by means of X-ray fluorescence spectrometry (XRF) using a Philips PW-1410 XRF spectrometer after the fusion of the Li borate.

For trace and rare-earth element analysis, samples were processed using ICP-MS with a four-acid method involving HF, HNO3, HCl, and HClO4. This procedure took two days in a fume hood using perchloric acid. Powder samples were also heated for six hours at 1000°C to determine the loss on ignition (LOI).

Results

Mineralogy

The results of the mineralogical analysis of carbonate components from the Sargelu Formation are shown in Table 1. The primary minerals in the two sections are calcite, dolomite, and quartz. Some samples also contain pyrite and feldspar, while others include hematite, pyrite, and albite. The clay component is rich in illite. These results show that the mineral compositions of the carbonate components differ between the two locations.

Table 1. Mineralogical composition of carbonate component, sargelu formation

Sample	Non-clay minerals (wt%)								Clay minerals (wt %)
	Quartz	Dolomite	Orthoclase	Calcite	Gypsum	Hematite	Pyrite	Albite	Illite
Bz1	17	25	3	48	1	1			4
Bz2	19	22	3	52		1			2
Bz3	21	21	4	47	2	1	1		3
Bz4	7	24	3	60	2				3
Bz5	15	21	4	55	1				3
Bz6	14	18	3	58	2				4
Bz7	17	33	4	40	2				3
Bz8	22	18	4	53	1				2
Bz9	15	19	3	57	1				4
Bz10	19	20	2	56					2
Bz11	21	19	3	55	1				1
Brs1	11	2	3	83					
Brs2	10	40	3	42					4
Brs3	18	32	4	43					2
Brs4	11	29	4	54			1		
Brs5	26	18	4	51					
Brs6	22	28	5	37				3	4
Brs7	5	38	5	49				2	
Brs8	8	37	3	45				3	3
Brs9	9	34	3	51				2	1
Brs10	7	38	2	48				3	2

This table 1. will show the mineralogical composition of the samples of carbonate components in the Sargelu Formation, both non-clay minerals and clay minerals. The table is divided into two sections, namely, non-clay minerals (quartz, dolomite, orthoclase, calcite, gypsum, hematite, pyrite, and albite) and clay minerals (including illite, which is predominant). In the case of the Barzewa (Bz1-Bz11) and Barsirin (Brs1-Brs10) sections, calcite, dolomite, and quartz form the major non-clay minerals. The most common non-clay mineral is calcite, which usually constitutes 40 to 60 % in both parts. There is also high dolomite content, especially in

the samples found in Barsirin, with a range of dolomite content ranging between 18% and 40%. The content of quartz is different, with the Barsirin samples ranging between 14% and 22%, and the Barzewa samples exhibiting a similar variation. Regarding clay minerals, the most common clay mineral in all of them is illite, the content of which ranges between 2% and 4% in both parts. Pyrite, hematite, albite, and orthoclase are present in small quantities in some samples, especially those found in Barsirin. It is interesting to note that the pyrite is present in a number of samples of both sections, and this may be a sign of the conditions under which it is deposited during its deposition process, which is that of a reducing environment. All in all, there are differences in the mineral compositions between the two sections (Barzewa and Barsirin), whereby the Barsirin samples were more inclined towards higher concentrations of dolomite and a more pronounced percentage distribution of hematite, pyrite, and albite. This indicates that there are variations in the depositional environment or diagenetic conditions in the two localities (Murris, 1980).

Fourier Transform Infrared (FTIR)

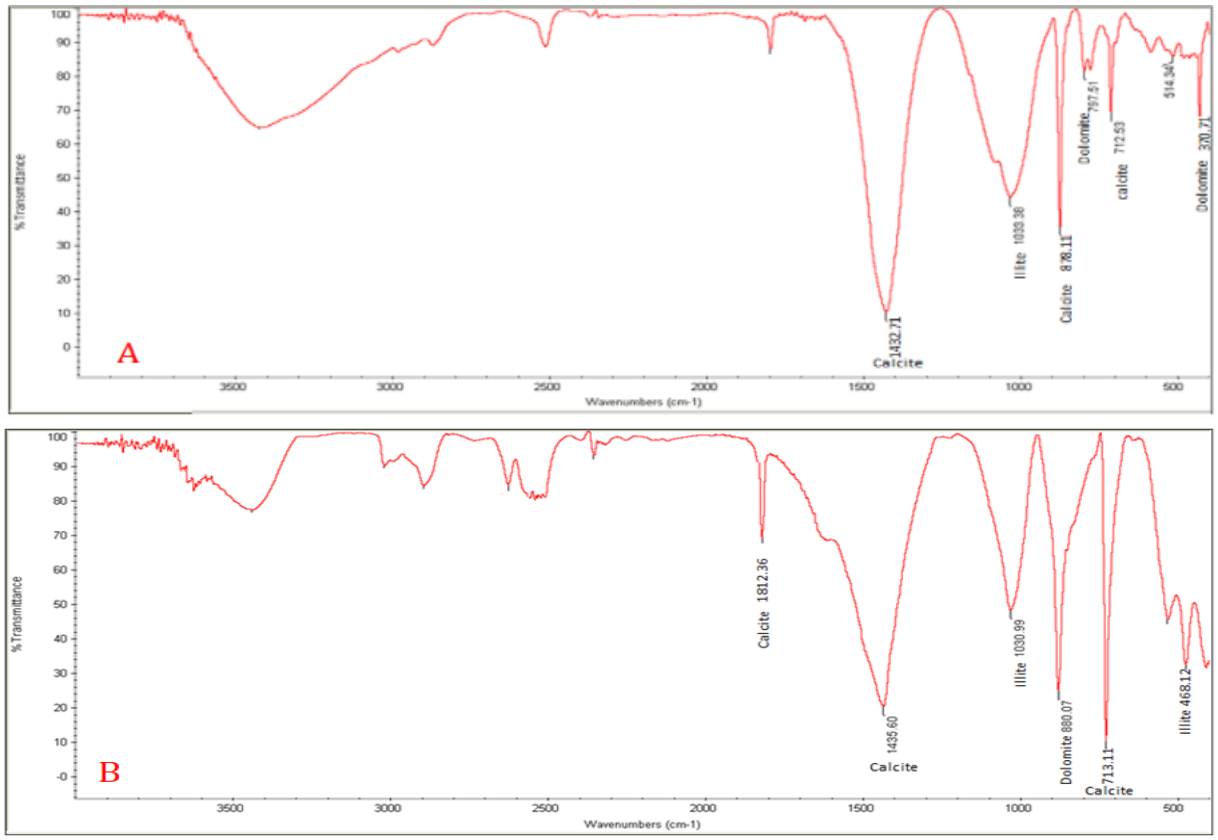

Figure 3. Infrared (IR) spectra of carbonate samples from the barzewa and barsarin sections of the sargelu formation, analyzing the wavelength range of 500 to 3500 cm-1

(A) IR spectrum of the Barzewa section (Bz4) with distinctive absorption peaks of calcite at 1812cm^{-1}, 1435 cm^{-1}, 878 cm^{-1}, and 713 cm^{-1}. Additional peaks are also located at 1021 cm^{-1}, 72 cm^{-1}, and 514cm^{-1}, which are also indicative of illite and dolomite.

(B) IR spectrum at the Barsarin part (Brs7) showing sharp peaks at calcite 1821 cm^{-1} and 1435 cm^{-1}. Other minerals also present in the spectrum are dolomite, 880 cm^{-1} and 371cm^{-1}, and illite, 1039 cm^{-1} and 468 cm^{-1}.

The spectra hold crucial details concerning the mineralogical composition of the carbonate samples in the context of the presence of calcite, dolomite, and illite. These sharp peaks of wavenumbers are the affirmation of the existence of these minerals in both parts which is illustrated in Figure 3.

Geochemistry

Major Oxides

This Table 2, shows the chemical abundances of principal oxides in the carbonate components from both the Barzewa (Bz1–Bz11) and Barsirin (Brs1–Brs10) sections of the Sargelu Formation. The table presents the weight percentages (wt %) of oxides including SiO_2 (silicon dioxide), Al_2O_3 (aluminum oxide), Fe_2O_3 (iron oxide), CaO (calcium oxide), MgO (magnesium oxide), Na_2O (sodium oxide), K_2O (potassium oxide), TiO_2 (titanium oxide), MnO (manganese oxide), P_2O_5 (phosphorus pentoxide), and LOI (loss on ignition).

Table 2. Major oxides (wt%) in carbonate components of the sargelu formation

Sample	SiO_2	Al_2O_3	Fe_2O_3	CaO	MgO	Na_2O	K_2O	TiO_2	MnO	P_2O_5	LOI	Total	Al_2O_3/TiO_2	SiO_2(wt%)[a]
Bz1	6.387	1.641	1.362	45.332	5.926	0.01	0.744	0.086	0.013	0.145	38.09	99.92	19.08	62.92
Bz2	9.621	2.517	1.666	34.577	10.704	0.00	1.027	0.164	0.014	0.123	39.38	99.64	15.04	57.93
Bz3	8.476	6.238	1.305	39.213	9.147	0.032	1.090	0.204	0.015	0.157	33.86	99.74	15.87	58.96
Bz4	8.179	2.022	1.470	40.652	9.076	0.068	0.847	0.123	0.016	0.190	37.45	99.94	15.20	58.12
Bz5	10.403	2.841	1.137	44.162	9.158	0.087	0.649	0.113	0.015	0.202	31.23	99.99	16.29	59.48
Bz6	8.689	4.332	2.034	43.457	8.206	0.161	1.217	0.258	0.011	0.159	31.00	99.52	16.79	60.09
Bz7	6.450	1.458	1.316	43.541	5.194	0.061	0.594	0.102	0.014	0.148	40.75	99.63	14.29	57.01
Bz8	8.687	1.661	1.362	41.232	7.926	0.01	0.634	0.086	0.012	0.244	38.19	99.92	19.08	62.92
Bz9	9.689	6.332	2.034	42.457	6.206	0.161	1.217	0.258	0.011	0.159	31.00	99.52	16.79	60.09
Bz10	8.079	2.021	1.580	41.662	8.086	0.058	0.737	0.133	0.016	0.130	37.53	99.94	15.20	58.12
Bz11	10.433	3.617	1.555	35.657	9.604	0.11	1.027	0.184	0.017	0.143	38.08	99.64	15.04	57.93
Brs1	7.450	10.886	4.249	35.790	7.769	0.106	4.438	0.809	0.028	0.398	25.98	99.90	17.16	60.56
Brs2	9.392	7.235	4.084	33.044	7.664	0.032	3.445	0.445	0.026	0.780	32.43	98.58	16.26	59.44
Brs3	9.028	6.103	2.156	38.881	9.875	0.029	1.253	0.129	0.020	0.586	30.82	99.95	22.33	66.94
Brs4	8.470	2.211	1.539	39.873	7.694	0.053	1.232	0.114	0.012	0.296	38.04	99.53	19.39	63.31
Brs5	9.316	5.880	2.119	37.453	6.223	0.083	1.835	0.222	0.028	0.394	37.35	99.90	17.48	60.94
Brs6	7.457	3.108	1.549	38.128	9.667	0.00	1.042	0.123	0.010	0.175	38.70	99.96	17.14	60.52
Brs7	9.151	3.475	1.652	41.411	8.632	0.058	1.331	0.183	0.021	0.331	35.66	99.44	19.43	63.35
Brs8	8.542	4.906	1.913	44.213	7.435	0.106	1.258	0.186	0.020	0.275	30.38	99.23	15.62	58.65
Brs9	7.038	5.114	2.276	44.891	8.897	0.029	1.253	0.139	0.030	0.576	30.82	99.95	22.33	66.94
Brs10	9.241	5.675	1.652	37.877	7.432	0.058	1.441	0.184	0.021	0.421	35.56	99.44	19.43	63.35
Average	8.58	4.251	1.905	40.167	8.120	0.062	1.348	0.202	0.018	0.287	34.871	99.76	17.392	60.836

Based on the results, calcium oxide (CaO) is the most dominant oxide, with an average of 40.17, silicon dioxide (SiO_2) 8.58, and magnesium oxide (MgO) 8.12. Aluminum oxide (Al_2O_3) has an average of 4.25 percent content, and the level of titanium oxide (TiO2) is moderate. It can also be seen that the data is correlated with Al_2O_3 and TiO_2, which suggests that there is some relationship between these oxides and the detrital phases in the samples. Also, there are direct correlations between Fe_2O_3, MnO, K_2O, and P_2O_5 and TiO_2, which also indicates these elements belong to detrital elements. The inverse relationship between CaO and SiO_2, Al_2O_3, Fe_2O_3, K_2O, and TiO_2 reflects the rise of carbonate phases at the expense of detrital phases. The overall level of the Al_2O_3/TiO_2 ratio of all the samples is 17.39, which means that the source rocks are in the form of an intermediate.

Trace Elements

The following table 3, shows the levels of trace elements (in parts per million, ppm) in the carbonate components of the Barzewa (Bz1 -Bz11) and Barsarin (Brs1 -Brs10) sections of the Sargelu Formation. These aspects are analyzed as the elements of strontium (Sr), uranium (U), vanadium (V), nickel (Ni), zinc (Zn), and

others, as well as average values of each part and the average of both parts of Barzewa and Barsarin. The carbonate contents of the Sargelu Formation have an exceptionally high level of strontium (Sr), with the mean standing at 357.28 ppm, and this is very similar to the Upper Continental Crust (UCC) value of 350 ppm but higher than the value of the Post-Archean Australian Shale (PAAS) at 200 ppm. Uranium (U) has a content of 17.3 ppm, 3.1 ppm, and 2.8 ppm in the PAAS and UCC, respectively. Conversely, the trace elements that include hafnium (Hf), cobalt (Co), thorium (Th), and even niobium (Nb) are more depleted in the Sargelu samples when compared to both UCC and PAAs.

Table 3. Trace element composition (ppm) of carbonate components from the barzewa and barsarin sections of the sargelu formation, with comparison to UCC and PAAS

Samples	Rb	Sr	Ba	Th	U	Y	Zr	Nb	Hf	Sc	V	Cr	Co	Ni	Cu	Zn	Th/U
Bz1	67.48	325.20	119.80	8.31	26.17	23.1	127.0	14.2	3.72	9.70	615.00	111.00	6.43	443.00	210.80	264.20	0.23
Bz2	31.20	219.50	56.10	1.55	22.33	21.1	17.00	1.06	0.44	3.90	671.00	77.00	4.29	535.00	146.10	312.40	0.05
Bz3	18.25	352.40	71.40	1.44	23.11	22.5	11.00	0.33	0.30	2.90	387.00	44.00	4.04	517.00	90.90	309.60	0.04
Bz4	15.30	370.70	54.30	1.09	12.76	13.2	12.00	0.26	0.27	2.20	128.00	22.00	0.94	243.00	63.00	101.30	0.05
Bz5	22.33	456.50	238.50	1.22	27.45	35.0	11.00	0.17	0.24	3.62	328.00	45.00	0.69	276.00	45.90	434.70	0.03
Bz6	18.51	373.50	122.70	0.60	22.17	15.8	3.00	0.76	0.04	2.10	197.00	25.00	0.31	286.00	43.10	135.90	0.02
Bz7	24.24	337.30	67.50	1.17	17.57	16.5	14.00	0.59	0.38	2.90	210.00	24.00	0.83	219.00	58.50	172.40	0.04
Bz8	22.42	390.30	84.10	1.28	16.80	25.0	13.00	0.23	0.33	3.40	194.00	30.00	1.28	281.00	54.60	90.20	0.05
Bz9	26.24	327.30	69.50	1.17	15.57	14.5	12.00	0.57	0.36	2.95	220.00	27.00	0.93	213.00	54.50	162.40	0.04
Bz10	63.48	315.20	109.80	7.31	24.17	21.1	137.0	13.2	3.62	9.90	625.00	121.00	6.33	463.00	200.80	274.20	0.21
Bz11	20.33	396.50	236.50	1.22	25.45	34.0	10.00	0.17	0.23	3.60	318.00	47.00	0.69	296.00	43.90	434.70	0.03
Av. Bz	29.98	351.31	111.84	2.39	21.23	21.98	33.36	2.86	0.90	4.29	353.91	52.091	2.43	342.90	92.01	244.72	0.08
Brs1	12.40	442.10	67.40	0.72	12.57	16.7	10.00	0.63	0.38	2.00	169.00	18.00	0.52	162.00	113.70	244.10	0.03
Brs2	25.81	293.70	76.80	1.42	10.65	18.5	18.00	1.79	0.58	3.00	312.00	26.00	1.19	221.00	47.60	225.30	0.07
Brs3	25.52	295.60	76.00	1.66	11.29	15.4	21.00	2.38	0.64	3.70	260.00	22.00	0.45	166.00	63.90	174.40	0.08
Brs4	15.76	448.10	97.20	1.24	9.00	16.0	15.00	1.37	0.49	2.60	230.00	26.00	0.95	167.00	30.50	201.90	0.07
Brs5	15.02	371.50	59.70	1.28	21.45	27.4	17.00	1.15	0.48	3.40	190.00	24.00	0.67	238.00	50.80	174.70	0.04
Brs6	27.75	327.90	93.00	1.83	16.82	31.9	25.00	2.48	0.70	4.80	563.00	42.00	0.43	511.00	63.30	438.20	0.07
Brs7	12.00	364.00	50.40	0.79	9.76	18.9	11.00	1.06	0.34	2.40	405.00	19.00	0.89	132.00	26.30	249.70	0.04
Brs8	25.75	337.90	95.00	1.93	14.82	30.9	26.00	2.58	0.80	4.90	583.00	41.00	0.53	501.00	61.30	428.20	0.08
Brs9	11.40	452.10	69.40	0.82	11.57	17.7	9.00	0.53	0.28	2.00	189.00	16.00	0.52	182.00	103.70	204.10	0.04
Brs10	26.52	305.60	77.00	1.76	10.29	14.4	22.00	2.48	0.74	3.80	270.00	24.00	0.25	186.00	61.90	184.40	0.09
Av. Brs	19.79	363.85	76.19	1.34	12.82	20.78	17.4	1.65	0.54	3.26	317.1	25.8	0.64	246.6	62.3	252.5	0.06
Total.Ave	94.86	357.28	94.86	1.89	17.23	21.41	25.76	2.28	0.73	3.79	336.38	39.57	1.58	297.05	77.86	248.43	0.07
UCC	112.00	350.00	550.00	10.7	2.80	22.0	190.0	25.00	5.80	11.0	60.00	35.00	10.0	20.00	25.00	71.00	3.82
PAAS	160.00	200.00	650.00	14.6	3.10	27.0	210.0	19.00	5.00	16.0	150.00	110.00	23.0	55.00	50.00	85.00	4.71
Norm.Sarg. fom	0.16	1.79	0.15	0.13	5.5	0.79	0.12	0.12	0.14	0.23	2.24	0.36	0.07	5.4	1.55	2.9	0.01
Nor. Bz	0.19	1.76	0.17	0.16	6.8	0.81	0.16	0.15	0.18	0.27	2.36	0.47	0.11	6.23	1.8	2.88	0.02
Nor. Brs	0.12	1.82	0.12	0.09	4.14	0.77	0.08	0.09	0.1	0.2	2.11	0.23	0.03	4.5	1.25	2.97	0.01
Nor. Ucc	0.7	1.75	0.85	0.73	0.90	0.81	0.90	1.31	1.16	0.69	0.4	0.32	0.43	0.36	0.50	0.83	0.81

Norm.Sarg.fom = normalized elements of Sargelu Formation. Nor. Bz = normalized elements of Barzewa section. Nor. Bz = normalized elements of Barserin section.

The average concentration of vanadium (V) in the Sargelu carbonates is 336.38 ppm, which is significantly above the values in PAAS (150 ppm) and UCC (60 ppm). Other important elements, such as nickel (Ni), zinc (Zn), rubidium (Rb), barium (Ba), copper (Cu), chromium (Cr), zirconium (Zr), and yttrium (Y), exhibit different concentrations among the samples. The normalized trace element results of the Sargelu Formation, Barzewa, and Barsarin sections have also been compared to the PAAS and UCC in the table. The given comparison assists in identifying differences in the trace element distribution that may serve as a valuable source of information on the geochemical properties of the Sargelu Formation and its possible origin.

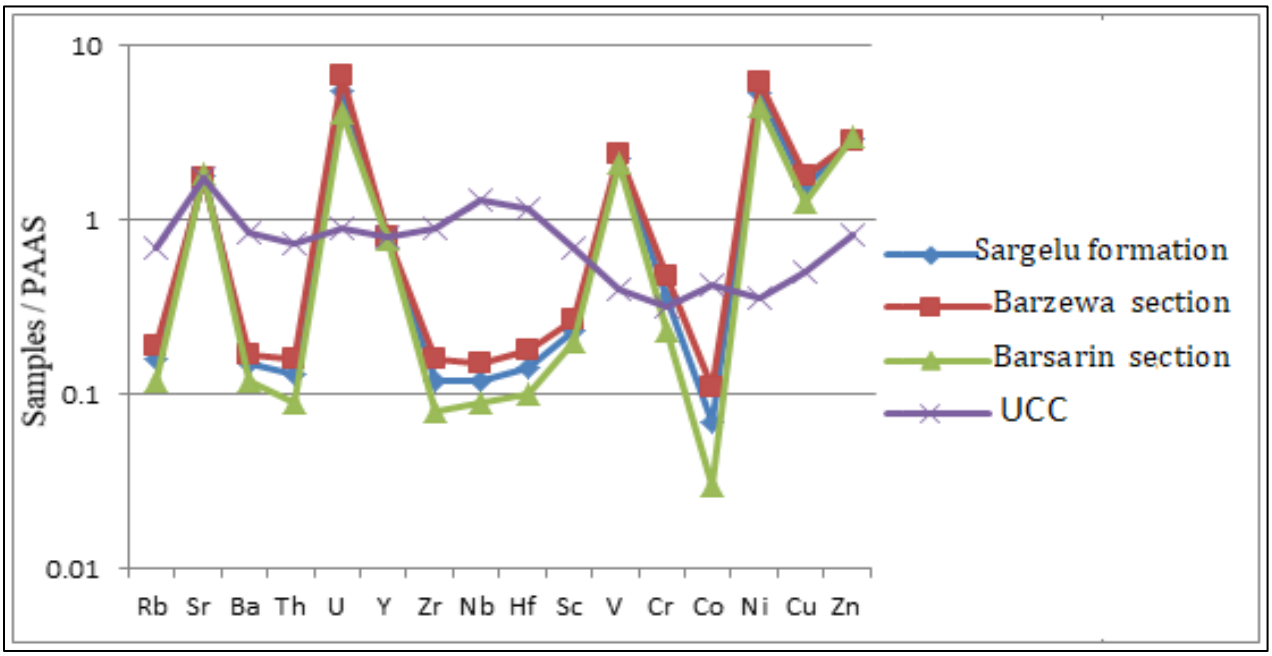

Figure 4. PAAS normalized trace element concentrations of carbonate components in the sargelu formation, barzewa section, and barsarin section compared to UCC (PAAS values after Taylor, 1985; Hull et al., 2020)

The Figure 4, is a comparison of the concentrations of the trace elements in the samples of the carbonate of the Sargelu Formation (blue line), the samples of the Barzewa section (red squares), the Barsarin section(green triangles), and the sample of the Upper Continental Crust (UCC) (purple stars) relative to the Post-Archean Australian Shale (PAAS). Essential variations in the concentrations of the trace elements in the two sections of the Sargelu Formation between the Barzewa and Barsarin sections can be found in the graph, which illustrates that the trace elements of the two sections are distinct. Some of them, e.g., strontium (Sr), vanadium (V), and uranium (U), are more concentrated in the two parts of the Sargelu Formation than in UCC. Conversely, the content of such elements as hafnium (Hf), cobalt (Co), and thorium (Th) is relatively less. This comparison gives more insight into the geochemical distinction between the carbonate in the Barzewa and the Barsarin parts of the Sargelu Formation and gives a more reasonable picture of how they relate to the values of the world crust.

Rare Earth Elements

The table 4, below displays the concentration levels of the rare-earth elements (REE) of samples of carbonates collected in the Barzewa (Bz1-Bz11) and the Barsarin (Brs1-Brs10) section of the Sargelu Formation in parts per million (ppm). The table includes key REEs such as lanthanum (La), cerium (Ce), praseodymium (Pr), neodymium (Nd), samarium (Sm), europium (Eu), gadolinium (Gd), terbium (Tb), dysprosium (Dy), holmium (Ho), erbium (Er), thulium (Tm), ytterbium (Yb), and lutetium (Lu), along with the total REE content (Σ REE) for each sample, as well as the average for both sections (Barzewa and Barsarin).

Table 4. Rare-earth element (ree) composition (ppm) of carbonate components from the barzewa and barsarin sections of the sargelu formation, with comparison to ucc and paas

Sample/Element	La	Ce	Pr	Nd	Sm	Eu	Gd	Tb	Dy	Ho	Er	Tm	Yb	Lu	Σ REE
Bz1	25.3	73.3	6.3	21.2	4.5	0.6	3.4	0.7	2.6	0.7	1.7	0.3	1.6	0.3	143.12
Bz2	14.3	39.9	2.5	10.3	2.3	0.4	2.1	0.5	1.9	0.4	1.4	0.2	1.1	0.2	77.47
Bz3	18.6	30.9	3.3	13.0	2.9	0.5	2.6	0.6	2.0	0.5	1.4	0.2	1.1	0.2	77.86
Bz4	12.6	14.8	2.6	8.4	1.8	0.4	1.5	0.3	1.2	0.3	0.8	0.1	0.6	0.1	45.81
Bz5	16.0	23.1	4.2	17.2	4.0	0.6	3.3	0.8	2.9	0.7	2.1	0.3	1.6	0.3	77.31
Bz6	14.1	21.5	2.5	9.1	1.9	0.4	1.4	0.4	1.5	0.3	1.3	0.3	0.8	0.1	55.55
Bz7	14.2	22.7	2.8	10.2	2.3	0.5	1.9	0.5	1.7	0.4	1.2	0.2	0.9	0.2	59.61
Bz8	14.3	18.4	3.6	13.4	3.0	0.4	2.5	0.6	2.3	0.5	1.6	0.2	1.3	0.2	62.84
Bz9	26.2	74.3	5.3	20.6	4.6	0.5	3.3	0.7	2.7	0.6	1.8	0.3	1.5	0.3	142.12
Bz10	12.6	14.8	2.6	8.4	1.8	0.4	1.5	0.3	1.2	0.3	0.8	0.1	0.6	0.1	45.81
Bz11	13.2	22.5	2.3	9.0	1.9	0.5	1.6	0.4	1.4	0.4	1.1	0.2	0.9	0.1	55.45
Ave. BZS	16.5	32.38	3.45	12.8	2.82	0.47	2.3	0.53	1.95	0.46	1.38	0.2	1.1	0.19	76.63
Brs1	13.3	21.0	2.7	9.1	2.2	0.4	1.7	0.4	1.4	0.5	1.2	0.3	0.8	0.1	56.09
Brs2	17.4	23.2	2.7	11.3	2.3	0.4	2.1	0.6	1.8	0.3	1.5	0.3	1.2	0.3	65.11
Brs3	12.3	21.8	2.4	8.8	2.0	0.5	1.7	0.4	1.5	0.4	1.1	0.2	1.0	0.1	54.27
Brs4	13.8	16.6	2.4	8.3	1.8	0.4	1.4	0.3	1.4	0.3	1.3	0.4	0.7	0.3	50.51
Brs5	17.1	21.5	3.5	13.4	3.0	0.5	2.7	0.6	2.5	0.6	1.8	0.3	1.4	0.2	67.36
Brs6	21.5	38.8	4.2	16.7	3.8	0.4	3.4	0.8	3.1	0.7	2.3	0.4	1.9	0.3	98.82
Brs7	15.1	24.0	2.0	7.5	1.7	0.5	1.6	0.5	1.4	0.4	1.3	0.3	1.3	0.2	57.65
Brs8	14.3	20.0	2.6	9.3	2.0	0.4	1.8	0.4	1.6	0.4	1.1	0.2	0.9	0.1	55.09
Brs9	12.8	17.6	2.3	8.4	1.9	0.5	1.6	0.4	1.5	0.4	1.1	0.2	0.8	0.1	49.51
Brs10	16.4	24.2	2.8	10.4	2.4	0.6	2.0	0.5	1.9	0.4	1.4	0.2	1.1	0.2	64.66
Av.Brs	15.4	22.87	2.8	10.32	2.31	0.46	2.	0.5	1.81	0.44	1.41	0.28	1.11	0.2	61.92
T. Ave.	15.97	27.85	3.12	11.62	2.6	0.47	2.15	0.51	1.88	0.45	1.4	0.25	1.1	0.2	69.62
UCC	30.0	64.0	7.1	26.0	4.5	0.9	3.8	0.6	3.5	0.8	2.3	0.3	2.2	0.3	146.37
PAAS	38.2	79.6	8.8	33.9	5.6	1.1	4.7	0.8	4.7	1.0	2.9	0.4	2.8	0.4	184.76
Cond. Total	**43.5**	**29.1**	**22.77**	**16.34**	**11.26**	**5.4**	**7.03**	**8.8**	**4.9**	**5.29**	**5.6**	**7.02**	**4.4**	**5.25**	
Cond. BZS	44.96	**33.84**	**25.18**	**18**	**12.21**	**5.4**	**7.52**	**9.14**	**5.12**	**5.4**	**5.54**	**5.62**	**4.44**	**4.99**	
Cond.Brs	**42**	**23.89**	**20.44**	**14.51**	**10**	**5.4**	**6.53**	**8.62**	**4.75**	**5.17**	**5.66**	**7.86**	**4.47**	**5.25**	
Cond. UCC	**81.74**	**66.87**	**51.82**	**36.57**	**19.48**	**10.34**	**12.42**	**10.34**	**9.19**	**9.4**	**9.24**	8.43	**8.87**	**7.87**	
Cond. PAAS	**104.09**	**83.18**	**64.23**	**47.68**	**24.24**	**12.64**	**15.36**	**13.79**	**12.34**	**11.75**	**11.65**	**11.24**	**11.29**	**10.50**	
Conderite	**0.367**	**0.957**	**0.137**	**0.711**	**0.231**	**0.087**	**0.306**	**0.058**	**0.381**	**0.0851**	**0.249**	**0.0356**	**0.248**	**0.0381**	

Cond. Total = Chondrite normalized elements of the Sargelu formation.

Cond. BZS = Elements of the Barzewa section normalized by Chondrite.

Cond. Brs = Chondrite normalized elements of Barserin section.

The mean Σ REE content of the Barzewa section is 76.63 ppm, and the Barsarin section is 61.92 ppm, with a mean of both sections being 69.62 ppm. The individual values of REEs are also the highest in the Barzewa samples, with the highest concentration being 143.12 ppm in sample Bz1. A comparison of these REE concentrations (with other REE patterns of the Upper Continental Crust (UCC)) and Post-Archean Australian Shale (PAAS) indicates that the pattern in the Sargelu Formation is enriched in the light rare-earth elements (LREEs) compared to the heavy rare-earth elements (HREEs). It also demonstrates that the concentrations of the REE of the Sargelu Formation are smaller than those of PAAS and UCC. The comparison also brings out the consistency in the concentration of REE in the carbonate constituents of both portions.

This Figure 5 presents the chondrite-normalized rare-earth element (REE) concentrations for carbonate samples from the Sargelu Formation. The data from the Barzewa section (red squares), Barsarin section (green triangles), and Sargelu Formation as a whole (blue line) are compared to the normalized values of the Upper Continental Crust (UCC), Post-Archean Australian Shale (PAAS), and chondrite values (purple stars). The pattern in Chondrite normalized indicates an overwhelmingly high level of enrichment of light rare-earth elements (LREEs) in the Sargelu Formation carbonates, with a progressive decline of the level of enrichment in the atomic number toward the heavy rare-earth elements (HREEs). Both sections have a negative europium

(Eu) anomaly, which means that they exhibited a significant deviation from chondritic values. It indicates that the REE composition of the Sargelu carbonates may be considered to be affected by specific geochemical processes and that these effects could be due to depositional settings or the source rocks of these elements.

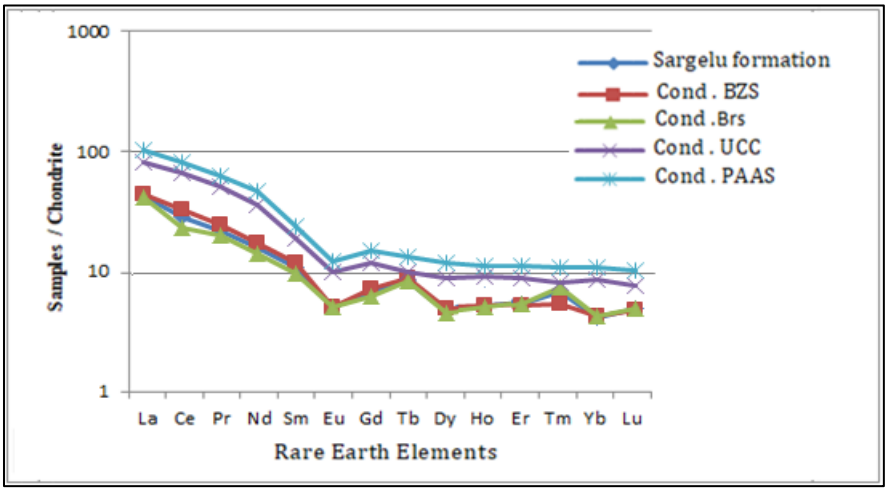

Figure 5. Chondrite normalized rare earth element (REE) concentrations of the carbonate components from the sargelu formation (chondrite normalized values from Taylor, 1985)

Discussions

Provenance (Composition of Source Area)

The composition of the source rocks embracing the Sargelu Formation has much information about its origin. In this paper, the ratio of Al_2O_3/TiO_2 is used as a leading indicator based on (Yamamoto et al., 1986), a well-established way of determining the immobility of such elements in the water body. A more accurate determination of the source rock composition can be made by this technique, mainly because Al_2O_3 and TiO_2 are not seriously fractionated during the transport of the sediment. Whereas the other studies have recognized the composition of source rocks, findings are different and show a more specific Al_2O_3/TiO_2 ratio of 17.39 (Table 2), which is a clear indication of the intermediate composition of the parent rocks. This is opposed to the previous research, where such a detailed geochemical study might not have been carried out due to the broad classification of source rocks in the past.

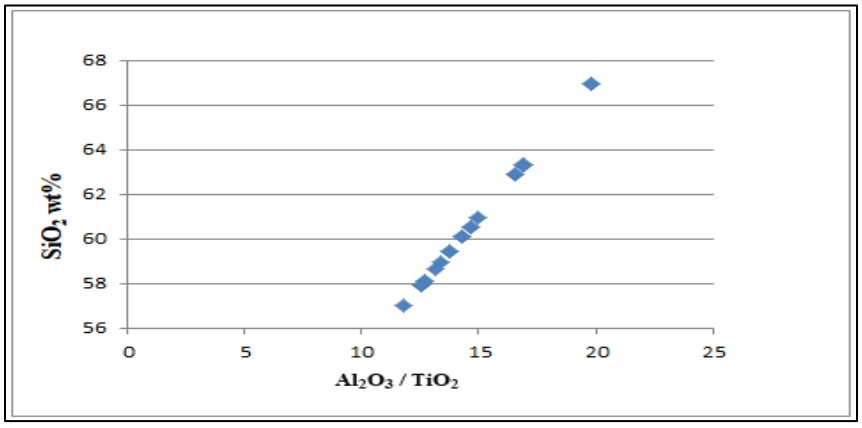

Figure 6. Increases Althe /Ti ratio gradually with increasing SiO_2 values of carbonate component Sargelu Formation, after (Moosavirad et al., 2011)

In addition, the fact that the ratio of Al/Ti rises proportionally with an increment in the level of SiO2 (Figure 6) indicates that the concentration level of alumina and titanium in these rocks is controlled by the presence of feldspars and mafic minerals such as biotite and pyroxene. This finding offers a more nuanced perspective on the tectonic and sedimentary history of the region, adding new knowledge compared to (Moosavirad et al., 2011) and others who have discussed the relationship between SiO2 and Al/Ti ratios but with less specificity regarding the intermediate composition of the Sargelu Formation's parent rocks.

Depositional Environment

V vs Al_2O_3 Diagram

The V vs Al2O3 diagram is an influential means that could be employed to differentiate between the various depositional settings, and the application of this diagram would contribute to the knowledge of the marine character of the Sargelu Formation. The level of V is low in freshwater deposits compared to that found in the marine environment; therefore, it is a good indicator of marine deposition (Mortazavi et al., 2014). The findings of plotting the carbonate samples on this diagram (Figure 7) show that the Sargelu Formation carbonates are grouped in both shallow and deep marine environments on sea ramps, as found in the previous research, but with a finer perspective. The past literature might have been able to assume the existence of shallow marine, but it did not provide the level of detail that such geochemical analysis could bring to differentiate these subtle differences in the depositional environments clearly. This difference between shallow and deep marine conditions introduces a novel understanding of the deposition history of the Sargelu Formation. Compared to other studies that may have generalized the environment, the use of this particular geochemical tool indicates the paramount place of sunlight in these marine environments and the differences between shallow and deep marine environments. The introduction of such a diagram adds more power to the interpretation of the depositional environment.

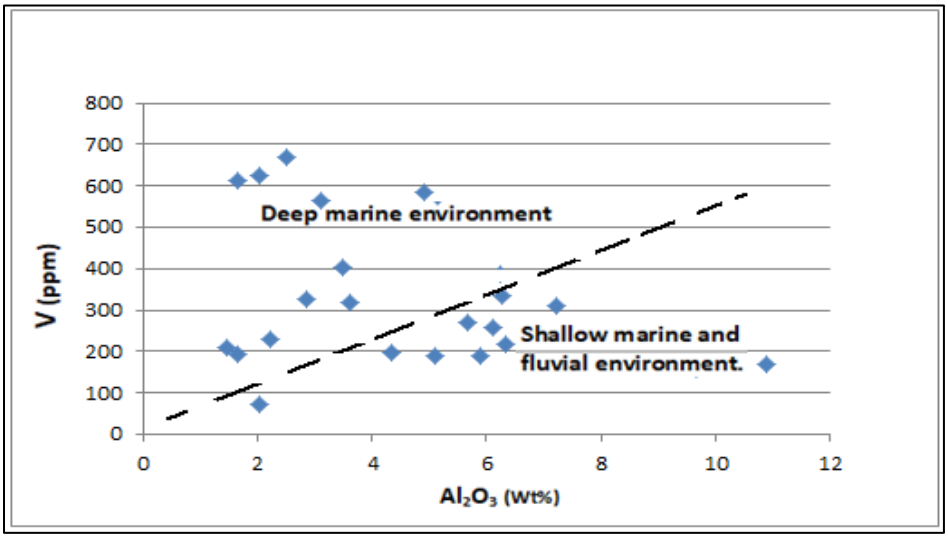

Figure 7. Plots of V vs Al_2O_3 diagram for carbonate continent of sargelu formation for paleoenvironmental depositional reconstruction after (Mortazavi et al., 2014)

Scanning Electron Microscope (SEM)

The paper contributes to the knowledge of the Sargelu Formation marine surroundings considerably due to the Scanning Electron microscope analysis (SEM) that you applied to examine the morphologies and textures of the carbonate minerals. This method allows for the identification of both euhedral and anhedral carbonates

such as calcite and dolomite (Figure 8). The coccoliths are also microscopic calcium carbonate plates that are formed by coccolithophores, as revealed in SEM. The marine character of the Sargelu Formation has been the subject of discussion in previous studies, but the discovery of coccoliths provides a new fine-tuning to the marine ecology of the formation.

Coccolithophores are unicellular calcifying algae that play a significant role in the marine carbon cycle, namely, the production of organic and carbonate carbon through photosynthesis and the calcification process, respectively (Hakimi et al.,2015). Coccolithophores, as Witer and Siesser (1994) propose, are important in the oceanic CO2 balance, and the coccoliths of the coccolithophores constitute a vital constituent of the deep-sea sediments. The discoveries provide some novel understanding of the presence of coccoliths in the marine ecosystem of the Middle Jurassic era, which were not explicitly covered in previous studies of the Sargelu Formation. This finding not only perfects the interpretation of the paleoenvironment but also creates an avenue in future studies concerning the carbon sinks and their applicability in explaining the global climate changes (Smith et al., 2012).

This novel information points out that coccolithophores thrived in the lighted areas of the ocean, which indicates that the sea was very productive during the Middle Jurassic. Furthermore, the discovery is also applicable in paleoceanography as it relates these microorganisms to the reconstructions of past environments to close the gaps in previous research that did not provide such detailed biological evidence.

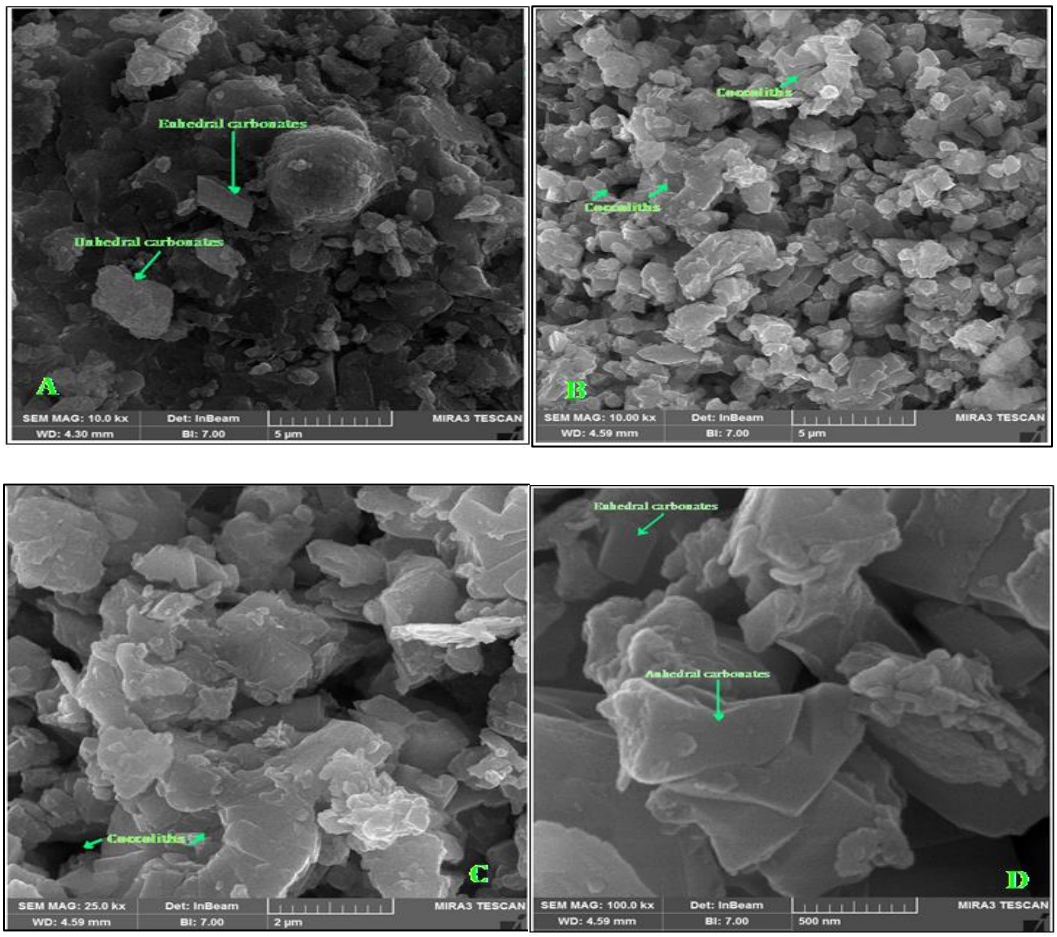

Figure 8. Scanning electron microscope (SEM) images showing carbonate microtextures from the sargelu formation at barzewa and barsarin sections (Müller, 2019)

(A, B) The Barzewa section exhibits predominantly euhedral carbonate crystals and coccolith structures, indicating well-preserved marine biogenic components within the carbonate matrix.

(C, D) The Barsarin section displays euhedral carbonate grains with distinct crystal morphology, reflecting secondary recrystallization and diagenetic overprinting.

These microstructures, such as the existence of coccoliths, ensure a marine setting of deposition and the role of coccolithophores in the carbonate sedimentation in the Middle Jurassic.

Contribution to Marine Environment Understanding

The findings are of great use in the study of the marine environment of the Sargelu Formation as they combine mineralogical and geochemical data with a close-up microstructural study (e.g., SEM). The past research used a single approach, be it the geochemistry or the mineralogical features, but the multidimensional approach will give a whole picture of the deposit history of the formation. The incorporation of coccoliths as a testimony of marine planktonic life develops another aspect to the perception of ancient marine food webs, an essential aspect that cannot be ignored in any previous study.

This study connects the Sargelu Formation with the current topic of climate change by highlighting the use of coccoliths as a carbon sink. The new coccolithophore ecological information in the Middle Jurassic provides yet another understanding of the biogeochemical cycles in the world, which is in itself a significant addition to the existing literature that did not directly address the ecological functions of these organisms.

Conclusion

The paper gives geochemical and mineralogical analysis of the Sargelu Formation, carbonate components of two parts of the formation of Barzewa and Barsarin of the northeastern governorate of Erbil in Iraq. Inorganic geochemistry (principal oxides, trace elements, and rare-earth elements), mineralogical methods (X-ray diffraction (XRD), Fourier-transform infrared (FTIR) spectroscopy, and Scanning Electron Microscopy (SEM)) can be used to make new discoveries on mineral composition and the context of deposition of these carbonates. Significant findings of this study are that the most outstanding mineral constituents, which are calcite, dolomite, quartz, and clay minerals, were found in the two sections. There was an SME analysis that indicated that the carbonate minerals are primarily euhedral and anhedral calcite and dolomite, which is very significant in the analysis of the mineralogical textures. Moreover, the paper also brings out the phenomenon of coccoliths to demonstrate that there is a shallow marine environment of deposition that is characterized by the presence of sunlight, which enhances planktonic food webs in the temperate and tropical oceans. Notably, the outcomes of the geochemical analysis reveal that the Sargelu Formation source rocks are of an intermediate nature, with the ratio of Al_2O_3/TiO_2 equal to 17.39, which is peculiar to both felsic and mafic source rocks. It gives important data on the place of origin and the process of sediment transportation that formed these carbonate rocks. The V vs Al_2O_3 diagram is also used to define the depositional environment of the study to show that the Sargelu Formation was deposited in the shallow seas with a few freshwater interferences. The publication is founded upon and develops previous literature, such as mineralogical and geochemical data that depict SEM analysis, in order to give a deeper understanding of the carbonate component of the Sargelu Formation, particularly of the mineralogical and geochemical signature of the Barzewa and Barsarin sections. The findings are significant as they provide a better representation of the deposition scenario and the materials that were involved in the Sargelu Formation, which contributes to the idea of learning more about what the marine regimes of the Middle Jurassic were in northeastern Iraq.

Acknowledgments

The authors extend their sincere gratitude to the Department of Earth Sciences and Petroleum, College of Science, Salahaddin University, Erbil, Kurdistan Region, Iraq, and the Chemical and Petrochemical Department, College of Engineering, Salahaddin University, Erbil, Iraq, for their continuous support and for providing the necessary laboratory facilities and academic guidance that made this study possible.

Author contribution

All the authors contributed equally.

Conflict of Interest

The authors declared that no conflict of interest.

Data Availability Statement

The data that support the findings of this study are currently not publicly available, as the manuscript is under review and the study has not yet been published. However, the data may be made available from the corresponding author upon reasonable request.

Ethical Considerations

No human subjects, animal experiments, or other personal confidential information were used in this study. Thus, there was no necessity to have ethical approval. All methods and procedures used in this study comply with institutional, national, and international guidelines and regulations applicable to the field of research. The authors affirm that there are no ethical conflicts or issues associated with this work.

Funding

This research received no specific grant from any funding agency in the public, commercial, or not-for-profit sectors. The author's respective institutions supported the work through internal resources and academic collaboration.

References

Abdula, R. A., Balaky, S. M., Nurmohamadi, M. S., & Piroui, M. (2015). Microfacies analysis and depositional environment of the Sargelu Formation (Middle Jurassic) from Kurdistan Region, northern Iraq. *Donnish Journal of Geology and Mining Research*, *1*(1), 001-026.

Al-Ameri, T. K., & Al-Nagshbandi, S. F. (2015). Age assessments and palynofacies of the Jurassic oil source rocks succession of North Iraq. *Arabian Journal of Geosciences*, *8*(2), 759-771. https://dx.doi.org/10.1007/s12517-013-1245-2

Al-Ameri, T. K., & Zumberge, J. (2012). Middle and upper Jurassic hydrocarbon potential of the Zagross fold Belt, North Iraq. *Marine and Petroleum Geology*, *36*(1), 13-34. https://doi.org/10.1016/j.marpetgeo.2012.04.004

Beydoun, Z. R. (1986). The petroleum resources of the Middle East: a review. *Journal of Petroleum Geology*, *9*(1), 5-27. https://doi.org/10.1111/j.1747-5457.1986.tb00370.x

Beydoun, Z. R., Clarke, M. H., & Stoneley, R. (1992). Petroleum in the Zagros Basin: a late Tertiary foreland basin overprinted onto the outer edge of a vast hydrocarbon-rich Paleozoic-Mesozoic passive-margin shelf. https://doi.org/10.1306/M55563C12

Chatterjee, R., & Singh, V. (2023). Net-Zero Cities: A Comparative Analysis of Decarbonization Strategies in Urban Planning. *International Journal of SDG's Prospects and Breakthroughs*, 1(1). 11-14.

Dai, L. Q., Zhao, Z. F., Zheng, Y. F., & Zhang, J. (2015). Source and magma mixing processes in continental subduction factory: Geochemical evidence from postcollisional mafic igneous rocks in the D abie orogen. *Geochemistry, Geophysics, Geosystems*, *16*(3), 659-680. https://doi.org/10.1002/2014GC005620

Ganesan, A., Sethuraman, P., & Balamurugan, S. (2024). The Impact of Geology on Environmental Management in Mining Operations. *Archives for Technical Sciences*, *2*(31), 86-93. https://doi.org/10.70102/afts.2024.1631.086

Hakimi, M. H., Mohialdeen, I. M., Abdullah, W. H., Wimbledon, W., Makeen, Y. M., & Mustapha, K. A. (2015). Biomarkers and inorganic geochemical elements of Late Jurassic-Early Cretaceous limestone sediments from Banik Village in the Kurdistan Region, Northern Iraq: implications for origin of organic matter and depositional environment conditions. *Arabian Journal of Geosciences*, *8*(11), 9407-9421.

He, J., Duan, Y., Zhang, X., Wu, B., & Xu, L. (2011). Hydrocarbon generation conditions of the shale in niutitang formation of lower cambrian, southern chongqing and northern Guizhou. *Marine Geology Frontiers*, *27*(7), 34-40.

Hull, P. M., Bornemann, A., Penman, D. E., Henehan, M. J., Norris, R. D., Wilson, P. A., Blum, P., Alegret, L., Batenburg, S. J., Bown, P. R., Bralower, T. J., Cournede, C., Deutsch, A., Donner, B., Friedrich, O., Jehle, S., Kim, H., Kroon, D., Lippert, P. C., . . . Zachos, J. C. (2020). On impact and volcanism across the Cretaceous-Paleogene boundary. *Science*, *367*(6475), 266–272. https://doi.org/10.1126/science.aay5055

Jassim, S. Z., & Goff, J. C. (Eds.). (2006). *Geology of Iraq*. DOLIN, sro, distributed by Geological Society of London. 15-115.

Kownacki, A., Szarek-Gwiazda, E., & Woźnicka, O. (2015). The importance of scanning electron microscopy (SEM) in taxonomy and morphology of Chironomidae (Diptera). *European Journal of Environmental Sciences*, *5*(1). https://doi.org/10.14712/23361964.2015.75

Majdanishabestari, K., & Soleimani, M. (2019). Using simulation-optimization model in water resource management with consideration of environmental issues. *International Academic Journal of Science and Engineering*, *6*(1), 15–25. https://doi.org/10.9756/IAJSE/V6I1/1910002

Martin, A. Z. (2001). Late Permian to Holocene paleofacies evolution of the Arabian Plate and its hydrocarbon occurrences. GeoArabia, 6(3), 445-504. https://doi.org/10.2113/geoarabia0603445

Moosavirad, S. M., Janardhana, M. R., Sethumadhav, M. S., Moghadam, M. R., & Shankara, M. (2011). Geochemistry of lower Jurassic shales of the Shemshak Formation, Kerman Province, Central Iran:

Provenance, source weathering and tectonic setting. *Geochemistry*, *71*(3), 279-288. https://doi.org/10.1016/j.chemer.2010.10.001

Mortazavi, M., Moussavi-Harami, R., Mahboubi, A., & Nadjafi, M. (2014). Geochemistry of the Late Jurassic–Early Cretaceous shales (Shurijeh Formation) in the intracontinental Kopet-Dagh Basin, northeastern Iran: implication for provenance, source weathering, and paleoenvironments. *Arabian Journal of geosciences*, *7*(12), 5353-5366.

Mousa, T. U. (2022). The Role of the Accounting Profession in Controlling Environmental Pollution According to Requirements of Social Responsibility in Industrial Companies. *International Academic Journal of Social Sciences, 9*(1), 29–42. https://doi.org/10.9756/IAJSS/V9I1/IAJSS0904

Müller, M. N. (2019). On the genesis and function of coccolithophore calcification. *Frontiers in Marine Science*, *6*, 49. https://doi.org/10.3389/fmars.2019.00049

Murris, R. J. (1980). Middle East: Stratigraphic evolution and oil habitat. *AAPG Bulletin*, *64* (5): 597–618 . https://doi.org/10.1306/2f918a8b-16ce-11d7-8645000102c1865d

Pitman, J. K., Steinshouer, D., & Lewan, M. D. (2004). Petroleum generation and migration in the Mesopotamian Basin and Zagros Fold Belt of Iraq: results from a basin-modeling study. *GeoArabia*, *9*(4), 41-72. https://doi.org/10.2113/geoarabia090441

Punam, S. R., & Patel, P. (2026). Integrating Soil Physics, Environmental Chemistry, and Computational Modeling: A Multidisciplinary Perspective on Heavy Metal Transport Using HYDRUS-1D. *Bridge: Journal of Multidisciplinary Explorations*, *2*(1), 1-9. https://doi.org/10.17051/JME/02.01.01

Smith, H. E., Tyrrell, T., Charalampopoulou, A., Dumousseaud, C., Legge, O. J., Birchenough, S., ... & Hydes, D. J. (2012). Predominance of heavily calcified coccolithophores at low CaCO3 saturation during winter in the Bay of Biscay. *Proceedings of the National Academy of Sciences*, *109*(23), 8845-8849. https://doi.org/10.1073/pnas.1117508109

Srinivas, G., & Rajesh, K. (2025). Hydrodynamic modeling of coastal erosion and its effect on marine ecosystems. *International Journal of Aquatic Research and Environmental Studies*, *5*(1), 354–373. https://doi.org/10.70102/IJARES/V5I1/5-1-35

TaylorSR, M. (1985). The continental crust: its composition and evolution. *Blackwell Scientific Publications, Oxford*, 1-328.

Van Bellen, R. C., & Dunnington, H. V. (1959). *Lexique stratigraphique international: Asie. Iraq*. Centre national de la recherche scientifique.

Yamamoto, K., Sugisaki, R., & Arai, F. (1986). Chemical aspects of alteration of acidic tuffs and their application to siliceous deposits. *Chemical Geology*, *55*(1-2), 61-76. https://doi.org/10.1016/0009-2541(86)90128-2